Indonesian Journal of Material Research
*e*-ISSN: 2987-1654
Vol. 1, No. 1, March 2023

Research Paper

# Biochar Derived from Rice Husk as Effective Adsorbent for the Removal Congo Red and Procion Red MX-5B Dyes

Alfan Wijaya[1], Nova Yuliasari[2]*

[1] *Research Centre of Inorganic Materials and Coordination Complexes, Faculty of Mathematics and Natural Sciences, Sriwijaya University, Palembang, 30139, South Sumatera, Indonesia*

[2] *Doctoral Program, Faculty of Mathematics and Natural Sciences, Universitas Sriwijaya, Jl. Padang Selasa No. 524 Ilir Barat 1, Palembang 30139, South Sumatera, Indonesia*

***Corresponding author**: nova_yuliasari@unsri.ac.id

**Abstract**

Biochar derived from rice husk was successfully prepared with the pyrolysis method. X-Ray Diffraction (XRD), Fourier-transform infrared spectroscopy (FT-IR), Thermogravimetry analysis (TGA), and Brunauer-Emmett-Teller (BET) analysis confirmed biochar. The results indicate that biochar is amorphous carbon. Functional groups on biochar include -OH, C-H, C-O, C=C, and C-O. The surface area of biochar of 72.252 $m^2/g$ with a pore size of 3.334 nm which is classified as mesoporous material. Biochar was used as an adsorbent on the congo red (CR) and procion red MX-5B (PR) dyes with adsorption capacities of 42.918 and 84.034 mg/g, respectively. The equilibrium adsorption occurred at 120 minutes. The adsorption isotherm and kinetics both followed the Langmuir isotherm and Pseudo Second Order (PSO), respectively. CR and PR adsorption process using biochar by physisorption and chemisorption with interactions that occur include hydrogen interactions, physical interactions, $\pi$-$\pi$ interactions, and electrostatic interactions.

**Keywords**

Biochar, Rice Husk, Adsorption, Congo Red, Procion Red MX-5B

Received: 3 January 2023, Accepted: 8 March 2023
https://doi.org/10.26554/ijmr.2023111

## 1. INTRODUCTION

The increase in rice production in each country will lead to an increase in rice husks which is an agricultural waste (Wang et al., 2023). Currently, in rice milling factories, many rice husks are disposed of directly to the ground and left to accumulate as biomass waste or burned. This will result in environmental pollution. Therefore, rice husk can be utilized in value-added products (Daffalla et al., 2020). Rice husk as one of the largest biomass wastes is good at producing renewable carbon and silica materials (Bai et al., 2021). One of the processes to obtain renewable carbon-based materials is the pyrolysis method. The product is named biochar (Abdullah et al., 2023). Biochar is a product of a low-cost pyrolysis process that can be obtained from various biomass wastes such as agricultural wastes. Biochar has chemical stability, porous structure, and adjustable physicochemical properties and is environmentally friendly, so biochar is recognized as an effective adsorbent for the remediation of various contaminants in wastewater (Liang et al., 2023; Liu et al., 2023).

One of the wastewaters that is commonly found in wastewater produced by the textile and paper industries contains dyes. Inadequate processing at various factories, and industrial effluents containing contaminated dyes in the waters will seriously harm the environment. Most dyes are not readily biodegradable and are toxic to aquatic life, even in small amounts (Rose et al., 2023). Dyes commonly found in wastewater are congo red (CR) and procion red-MX-5B (PR). Chemical structure of CR and PR shown in Figure 1. CR can cause bladder cancer and gene mutations if exposed to humans (Wang et al., 2022) and other health problems such as breathing difficulties, nausea, and diarrhea (Rose et al., 2023). PR is recognized as a carcinogenic and mutagenic agent that causes health problems in humans and aquatic life (Nazifa et al., 2018). Hence, the need to complete removal of dye from wastewater is necessary. Many researchers

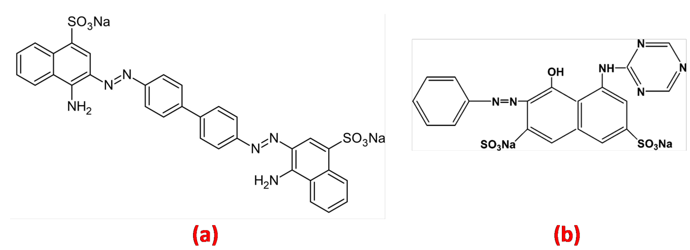


**Figure 1.** Chemical Structure of CR (a) and PR (b) Dyes

have investigated dye removal methods, however adsorption stands out as a popular method because of its high efficiency, environmental friendliness, operational simplicity, stability, and selectivity (Obayomi et al., 2023;Ahmad et al., 2023).

Research conducted by Nguyen et al. (2021), using biochar derived from agricultural waste (Acacia auriculiformis) modified with metal salts ($AlCl_3$) which resulted in an adsorption capacity of CR of 30.80 mg/g. Zhang et al. (2020) used biochar derived from Mango peel and applied to toxic heavy metal (cadmium) which resulted in a maximum capacity of 13.28 mg/g. Adsorption of methylene blue dye was carried out by Roy et al. (2022) using biochar derived from Citrus macroptera peel and produced a large adsorption capacity of 139.7 mg/g. Various studies have been conducted, proving that biochar applied as an adsorbent can be an effective and environmentally friendly material in the removal of contaminants in wastewater.

In this research, biochar will be prepared from rice husk and applied as adsorbent on CR PR dyes. Biochar was characterized using X-Ray Diffraction (XRD), Fourier-transform infrared spectroscopy (FT-IR), Thermogravimetry analysis (TGA), and Brunauer-Emmett-Teller (BET) analysis. Adsorption parameters to be studied include contact time variation (kinetic), concentration variation and temperature variation (isotherm and thermodynamics).

## 2. EXPERIMENTAL SECTION

### 2.1 Materials and Characterizations

Rice husk was collected from local farms in Palembang, South Sumatra, Indonesia. Distilled water ($H_2O$), procion red MX-5B (PR), and congo red (CR) dyes. Biochar was characterized using a Rigaku Miniflex-600 X-ray Diffractometer, Shimadzu Prestige-21 FTIR spectrophotometer, Quantachrome Instruments for BET surface area analysis, and Shimadzu Instruments for the thermogravimetric analyzer. Absorbance measurements of the dye's solution were conducted using a UV-Visible Biobase spectrophotometer UV BK-1800PC.

### 2.2 Preparation of Biochar Derived from Rice Husk

Water was used to wash the rice husk to get rid of impurities. A 100°C oven was used to dry the rice husk for 6 hours. Pyrolysis was used to create biochar, which was produced at 500°C for two hours. The collected samples were cleaned before being dried for ten hours at 100°C in an oven.

### 2.3 Adsorption Study

The process of adsorption required into account contact time, concentration, and temperature. By adjusting the contact duration (5, 10, 15, 20, 30, 50, 70, 90, 120, and 150 minutes) during adsorption, the impact of contact time on the adsorption of CR and PR dyes was quantified. An Erlenmeyer flask holding 20 mL of the dye solution at a concentration of 50 mg/L was added along with as much as 0.02 g of the adsorbent. A UV-visible spectrophotometer was used to measure the absorbance of the filtrate for the given time variation after the mixture had been agitated. The effects of the concentration (50, 60, 70, 80, 90 mg/L) and temperature (303, 313, 323, 333 K) were determined by varying these parameters during adsorption. As much as 0.02 g of the adsorbent was added to an Erlenmeyer flask containing 20 mL of the dye solution for a specified concentration variation and stirred for 60 minutes at the specified temperature. The absorbance of the filtrate was measured.

**Table 1.** BET Analysis Results

| Surface Area ($m^2/g$) | Pore Size (nm) | Pore Volume ($cm^3/g$) |
|---|---|---|
| 72.252 | 3.334 | 0.060 |

## 3. RESULTS AND DISCUSSION

The XRD pattern of the biochar derived from rice husk has been shown in Figure 2(a). Figure 2(a) shows a strong and broadened peak at 20° which indicates the presence of $SiO_2$. Silicon is widely contained in most rice husks (Islam et al., 2021). The peak range at $2\theta$ = 20° (002) with a broadened peak shape biochar is amorphous carbon (Le et al., 2021). Figure 2(b) shows the FTIR spectra of the biochar. From the results of the FTIR analysis in Figure 2(b), it was found that in biochar there are functional groups indicated in the peaks which include -OH (3449 $cm^{-1}$), C-H (2924 $cm^{-1}$), C-O (1620 $cm^{-1}$), C=C (1435 $cm^{-1}$), and C-O (1103 $cm^{-1}$) (Zhang et al., 2022).

**Table 2.** Comparison of Surface Area with Other Biochar

| Biochars | Pyrolysis Temperature (°C) | Surface Area ($m^2/g$) | References |
|---|---|---|---|
| Plantain peel | 600 | 16.69 | (Felix et al., 2018) |
| *Punica granatum* | 300 | 41.28 | (Cao et al., 2019) |
| Eggshell membrane | 300 | 8.484 | (Wu et al., 2022) |
| Orange Peel | 400 | 0.90 | (Zhang et al., 2022) |
| Fishbone | 538 | 32.138 | (Tan et al., 2023) |
| Rice husk | 500 | 72.252 | This research |

Thermogravimetry profile of biochar shown in Figure 2(c). The TGA profile of the biochar prominently exhibits three regions which start at 60-105 °C, indicating dehydration (Wu et al., 2022), the organic contents were degraded at 200-600 °C, and in the third region at >600 °C, the carbonaceous matters were degraded (Nithyalakshmi and Saraswathi, 2021). The $N_2$ adsorption/desorption isotherm of biochar shown in Figure 2(d). Based on the data in Figure 2(d), the BET isotherm type tends to approach type IV with the presence of hysteresis indicating

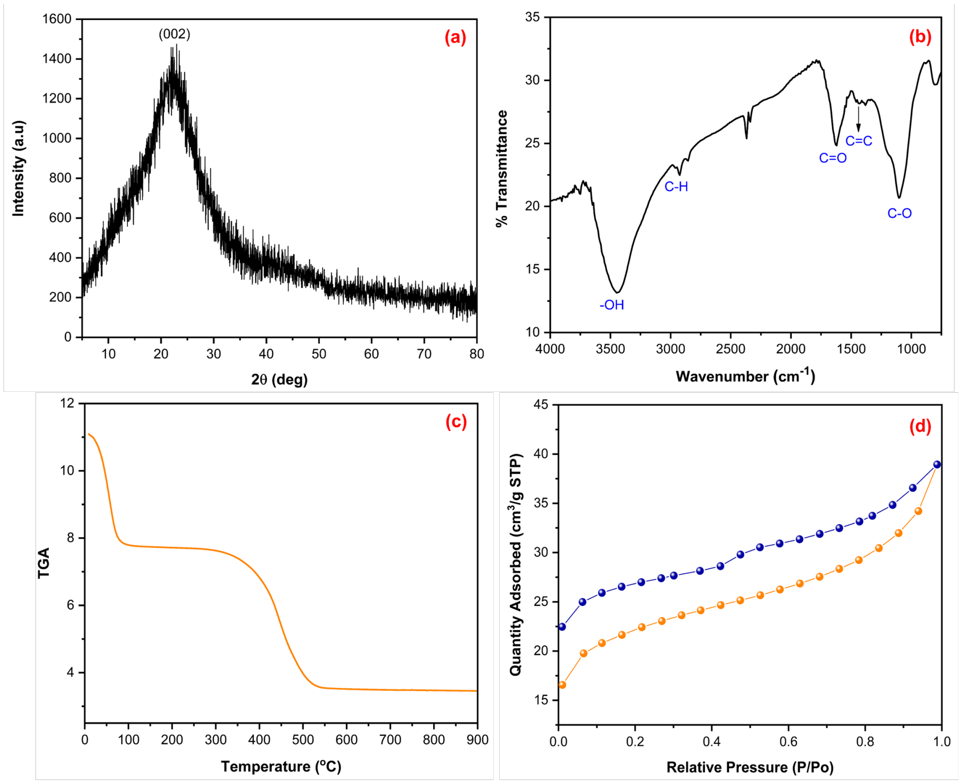


**Figure 2.** Biochar Characterization Results: XRD Diffractogram (a), FTIR Spectra (b), Thermogravimetry Profile (TGA) (c), and $N_2$ Adsorption/desorption Isotherm (d)

the presence of non-uniform material pores. The results of the BET analysis are shown in Table 1. The surface area of biochar obtained from rice husk produces a large value of 72.252 $m^2/g$. The pore size of biochar is 3.334 nm which is classified as mesoporous material. According to IUPAC, mesoporous materials are those with pore sizes between 2-50 nm. Table 2 shows the various materials converted into biochar by pyrolysis method at various temperatures that have been reported. From these data, the biochar derived from rice husk in this study has the characteristics of a larger surface area than other materials.

Figure 3 and Table 3 both display the effect contact time adsorption and kinetic parameters, respectively. After 120 minutes, CR reached equilibrium and underwent an insignificant rise in adsorption concentration. According to Table 3, the adsorption kinetics followed PSO, and the linear regression coefficient ($R^2$) value was close to 1. The PSO kinetics model assumes that the adsorption rate depends not on the adsorbate concentration but on the adsorption capacity, and the adsorption process occurs chemisorption.

Figure 4 depicts the impact of concentration and temperature on the adsorption of CR and PR. The rise in adsorption concentration is caused by rising temperature, as seen in Figure 4. In Table 4, isotherm adsorption was displayed. Table 4 displays the substantial adsorption capacity that occurred at adsorption temperatures of 313K for CR and 303K for PR, respectively, with adsorption capacities of 42.918 mg/g and 84.034 mg/g, respectively. Due to CR's bigger molecular weight and more complicated structure, PR has a higher adsorption capability than CR.

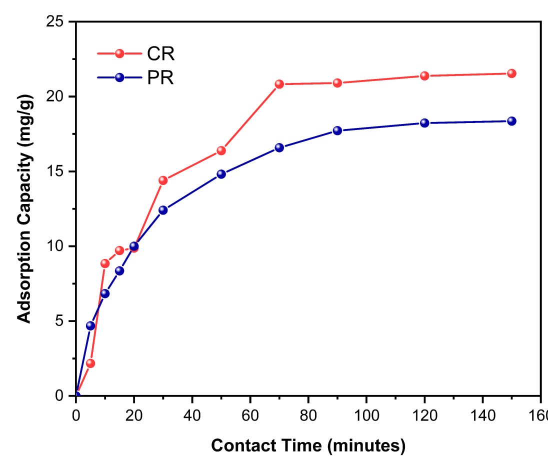


**Figure 3.** Effect Contact Time on Adsorption of CR and PR Dyes

In this study, the adsorption process is better described by the Langmuir model than by the Freundlich model, with an $R^2$ value that is closer to 1. Table 5 displays the thermodynamic parame-

 

**Table 3.** Kinetic Parameters

| Dyes | $Qe_{Exp}$ (mg/g) | Pseudo First Order (PFO) | | | Pseudo Second Order (PSO) | | |
|---|---|---|---|---|---|---|---|
| | | $Qe_{Calc}$ (mg/g) | $R^2$ | $k_2$ | $Qe_{Calc}$ (mg/g) | $R^2$ | $k_2$ |
| CR | 21.450 | 24.160 | 0.965 | 0.047 | 27.173 | 0.989 | 0.016 |
| PR | 18.354 | 17.254 | 0.984 | 0.034 | 20.747 | 0.998 | 0.002 |

**Table 4.** Isotherm Adsorption

| Dyes | Adsorption Isotherm | Adsorption Constant | T (K) | | | |
|---|---|---|---|---|---|---|
| | | | 303 | 313 | 323 | 333 |
| CR | Langmuir | Qmax | 42.735 | 42.918 | 42.735 | 42.735 |
| | | kL | 0.044 | 0.031 | 0.057 | 0.064 |
| | | $R^2$ | 0.979 | 0.980 | 0.982 | 0.989 |
| | Freundlich | n | 2.820 | 1.427 | 1.159 | 1.263 |
| | | kF | 7.323 | 2.734 | 1.943 | 2.690 |
| | | $R^2$ | 0.959 | 0.990 | 0.962 | 0.958 |
| PR | Langmuir | Qmax | 84.034 | 74.074 | 72.464 | 67.114 |
| | | kL | 0.030 | 0.043 | 0.060 | 0.093 |
| | | $R^2$ | 0.999 | 0.998 | 0.990 | 0.990 |
| | Freundlich | n | 1.815 | 2.192 | 2.446 | 3.085 |
| | | kF | 5.706 | 8.700 | 11.330 | 16.190 |
| | | $R^2$ | 0.998 | 0.990 | 0.980 | 0.980 |

**Table 5.** Thermodynamic Adsorption

| Dyes | T (K) | Qe (mg/g) | ΔH (kJ/mol) | ΔS (J/mol K) | ΔG (kJ/mol) |
|---|---|---|---|---|---|
| CR | 303 | 45.429 | 4.853 | 0.016 | -0.004 |
| | 313 | 46.778 | | | -0.165 |
| | 323 | 47.968 | | | -0.325 |
| | 333 | 49.397 | | | -0.485 |
| PR | 303 | 46.329 | 8.065 | 0.027 | -0.081 |
| | 313 | 48.101 | | | -0.350 |
| | 323 | 50.759 | | | -0.619 |
| | 333 | 52.658 | | | -0.887 |

**Table 6.** Adsorption Capacity of CR and PR Compared to Other Adsorbents

| Dyes | Adsorbents | Adsorption Capacity (mg/g) | References |
|---|---|---|---|
| CR | $AlCl_3$-biochar | 30.80 | (Nguyen et al., 2021) |
| | Polyvinyl alcohol/sodium alginate/ ZSM-5 zeolite membrane | 5.33 | (Radoor et al., 2020) |
| | Industrial waste (Fly ash) | 22.12 | (Harja et al., 2022) |
| | Pine bark | 3.92 | (Litefti et al., 2019) |
| | Untreated coffee husk | 38.65 | (Vairavel et al., 2021) |
| | Biochar (rice husk) | 42.918 | Present work |
| PR | Corncob activated carbon | 2.86 | (Nazifa et al., 2018) |
| | Cu-Al/Graphite | 49.505 | (Wijaya et al., 2021) |
| | Raw and acid-treated Montmorillonite K10 | 11.04 | (Sarma et al., 2018) |
| | Spent tea leaves | 3.28 | (Heraldy et al., 2016) |
| | Bentonite intercalated organometallic complex | 72.99 | (Vitanesa et al., 2017) |
| | Biochar (rice husk) | 84.034 | Present work |

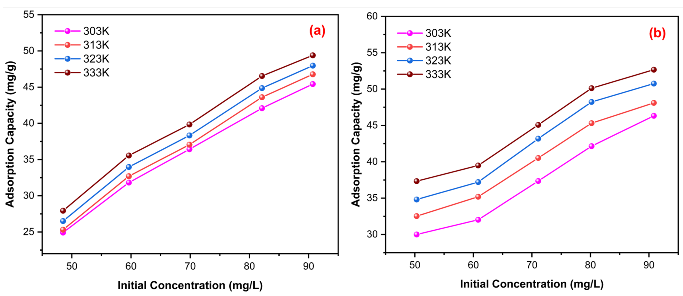


**Figure 4.** Effect of Concentration and Temperature on the Adsorption of CR (a) and PR (b) Dyes

ters for adsorption. The physical adsorption process is indicated by the enthalpy (ΔH) values of 4.853 and 8.065 kJ/mol. Enthalpy levels under 20 kJ/mol typically signify the physics of adsorption. Adsorption is an endothermic process with positive ΔH values, while ΔS values indicate that the degree of irregularity in the adsorption process is small.

A comparison of the adsorption capacity of CR and PR with other reported adsorbents is shown in Table 6. These data demonstrate the effectiveness of biochar in this study in the adsorption process of CR and PR. The greater the adsorption capacity produced indicates high effectiveness in the adsorption process. Based on the data presented in Table 6, it can be concluded that the biochar produced from rice husk in this study had a higher capacity for adsorption than other adsorbents in the CR and PR adsorption processes.

Schematic of CR and PR dye adsorption mechanism on biochar shown in Figure 5. Based on the kinetics model data, the adsorption process occurs chemically, while the small enthalpy value data indicates that adsorption occurs physically. Therefore, it can be concluded that the adsorption process takes place both,

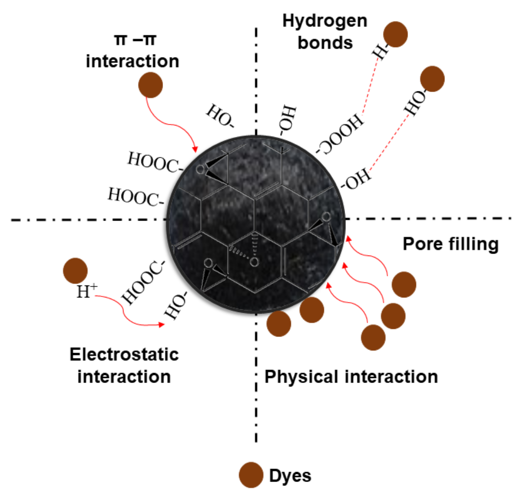


**Figure 5.** Schematic of CR and PR Dyes Adsorption Mechanism on Biochar

by physisorption and chemisorption. The interactions that occur in the adsorption process of CR and PR using biochar have been illustrated in Figure 6 which includes hydrogen interactions, physical interactions, $\pi$-$\pi$ interactions, and electrostatic interactions.

## 4. CONCLUSIONS

Biochar derived from rice husk was used as an adsorbent in the CR and PR adsorption process with adsorption capacities of 42.918 and 84.034 mg/g, respectively. The equilibrium adsorption occurred at 120 minutes. The adsorption isotherm and kinetics both followed the Langmuir isotherm and PSO, respectively. CR and PR adsorption process using biochar by physisorption and chemisorption with interactions that occur include hydrogen interactions, physical interactions, $\pi$-$\pi$ interactions, and electrostatic interactions.

## 5. ACKNOWLEDGEMENT

The authors thank to Research Centre of Inorganic Materials and Coordination Complexes FMIPA Universitas Sriwijaya for support and instrumental analysis.

## REFERENCES

Abdullah, N., R. M. Taib, N. S. M. Aziz, M. R. Omar, and N. M. Disa (2023). Banana Pseudo-stem Biochar Derived from Slow and Fast Pyrolysis Process. *Heliyon*; 12940

Ahmad, N., F. S. Arsyad, I. Royani, P. M. S. B. N. Siregar, T. Taher, and A. Lesbani (2023). High Regeneration of ZnAl/NiAl-Magnetite Humic Acid for Adsorption of Congo Red from Aqueous Solution. *Inorganic Chemistry Communications*, **150**; 110517

Bai, W., M. Qian, Q. Li, S. Atkinson, B. Tang, Y. Zhu, and J. Wang (2021). Rice Husk-based Adsorbents for Removing Ammonia: Kinetics, Thermodynamics and Adsorption Mechanism. *Journal of Environmental Chemical Engineering*, **9**(4); 105793

Cao, Q., Z. Huang, S. Liu, and Y. Wu (2019). Potential of *Punica granatum* Biochar to Adsorb Cu (II) in Soil. *Scientific reports*, **9**(1); 11116

Daffalla, S. B., H. Mukhtar, and M. S. Shaharun (2020). Preparation and Characterization of Rice Husk Adsorbents for Phenol Removal from Aqueous Systems. *PloS one*, **15**(12); 0243540

Felix, N., N. Ienna, İ. Ikelle, O. Anselm, E. Nwabueze, İ. Emeka, and O. Clinton (2018). Activated Plantain Peel Biochar As Adsorbent For Removal of Zinc (II) Ions From Aqueous Solution: Equilibrium and Kinetics Studies. *Journal of the Turkish Chemical Society Section A: Chemistry*, **5**(3); 1257–1270

Harja, M., G. Buema, and D. Bucur (2022). Recent Advances in Removal of Congo Red Dye by Adsorption Using an Industrial Waste. *Scientific Reports*, **12**(1); 6087

Heraldy, E., R. R. Osa, and V. Suryanti (2016). Adsorption of Procion Red MX 8B Using Spent Tea Leaves as Adsorbent. *AIP Conference Proceedings*, **1710**(1); 030025

Islam, T., C. Peng, I. Ali, J. Li, Z. M. Khan, M. Sultan, and I. Naz (2021). Synthesis of Rice Husk-derived Magnetic Biochar through Liquefaction to Adsorb Anionic and Cationic Dyes from Aqueous Solutions. *Arabian Journal for Science and Engineering*, **46**; 233–246

Le, P. T., H. T. Bui, D. N. Le, T. H. Nguyen, L. A. Pham, H. N. Nguyen, Q. S. Nguyen, T. P. Nguyen, N. T. Bich, and T. T. Duong (2021). Preparation and Characterization of Biochar Derived from Agricultural by-products for Dye Removal. *Adsorption Science and Technology*, **2021**; 1–14

Liang, H., W. Wang, H. Liu, X. Deng, D. Zhang, Y. Zou, and X. Ruan (2023). Porous MgO-modified Biochar Adsorbents Fabricated by the Activation of Mg $(NO_3)_2$ for Phosphate Removal: Synergistic Enhancement of Porosity and Active Sites. *Chemosphere*, **324**; 138320

Litefti, K., M. S. Freire, M. Stitou, and J. González-Álvarez (2019). Adsorption of an Anionic Dye (Congo Red) from Aqueous Solutions by Pine Bark. *Scientific Reports*, **9**(1); 1–11

Liu, Z., M. Jia, Q. Li, S. Lu, D. Zhou, L. Feng, Z. Hou, and J. Yu (2023). Comparative Analysis of the Properties of Biochars Produced from Different Pecan Feedstocks and Pyrolysis Temperatures. *Industrial Crops and Products*, **197**; 116638

Nazifa, T. H., N. Habba, A. Aris, and T. Hadibarata (2018). Adsorption of Procion Red MX-5B and Crystal Violet Dyes from Aqueous Solution onto Corncob Activated Carbon. *Journal of the Chinese Chemical Society*, **65**(2); 259–270

Nguyen, D. L. T., Q. A. Binh, X. C. Nguyen, T. T. H. Nguyen, Q. N. Vo, T. D. Nguyen, T. C. P. Tran, T. A. H. Nguyen, S. Y. Kim, and T. P. Nguyen (2021). Metal Salt-modified Biochars Derived from Agro-waste for Effective Congo Red Dye Removal. *Environmental Research*, **200**; 111492

Nithyalakshmi, B. and R. Saraswathi (2021). Removal of Colorants from Wastewater Using Biochar Derived from Leaf Waste. *Biomass Conversion and Biorefinery*; 1–17

Obayomi, K. S., S. Y. Lau, O. Ibrahim, J. Zhang, L. Meunier, M. M. Aniobi, B. T. Atunwa, B. K. Pramanik, and M. M. Rahman (2023). Removal of Congo Red Dye from Aqueous Environment by Zinc Terephthalate Metal Organic Framework Decorated on Silver Nanoparticles-loaded Biochar: Mechanistic Insights of Adsorption. *Microporous and Mesoporous Materials*, **355**; 112568

Radoor, S., J. Karayil, J. Parameswaranpillai, and S. Siengchin (2020). Removal of Anionic Dye Congo Red from Aqueous Environment Using Polyvinyl Alcohol/sodium Alginate/ZSM-5 zeolite Membrane. *Scientific reports*, **10**(1); 1–15

Rose, P. K., R. Kumar, R. Kumar, M. Kumar, and P. Sharma (2023). Congo Red Dye Adsorption onto Cationic Amino-modified Walnut Shell: Characterization, RSM Optimization, Isotherms, Kinetics, and Mechanism Studies. *Groundwater for Sustainable Development*, **21**; 100931

Roy, H., T. R. Prantika, M. Riyad, S. Paul, and M. S. Islam (2022). Synthesis, Characterizations, and RSM Analysis of Citrus macroptera Peel Derived Biochar for Textile Dye Treatment. *South African Journal of Chemical Engineering*, **41**; 129–139

Sarma, G. K., S. SenGupta, and K. G. Bhattacharyya (2018). Adsorption of Monoazo Dyes (Crocein Orange G and Procion Red MX5B) from Water Using Raw and Acid-treated Montmorillonite K10: Insight into Kinetics, Isotherm, and Thermodynamic Parameters. *Water, Air, and Soil Pollution*, **229**; 1–17

Tan, C., X. Zhang, C. Liao, Y. Huang, J. Zheng, H. Chen, and H. He (2023). Optimization of Fishbone Biochar Preparation Process Based on Adsorption Performance. *Sustainable Chemistry and Pharmacy*, **32**; 101015

Vairavel, P., N. Rampal, and G. Jeppu (2021). Adsorption of Toxic Congo Red Dye from Aqueous Solution Using Untreated Coffee Husks: Kinetics, Equilibrium, Thermodynamics and Desorption Study. *International Journal of Environmental Analytical Chemistry*; 1–20

Vitanesa, L., R. N. Purba, A. Lesbani, and M. Said (2017). Bentonite Intercalated Organometallic Complex as Adsorbent of Procion Red. *Science and Technology Indonesia*, **2**(1); 9–16

Wang, H., W. Luo, R. Guo, D. Li, and B. Xue (2022). Effective Adsorption of Congo Red Dye by Magnetic Chitosan Prepared by Solvent-free Ball Milling. *Materials Chemistry and Physics*, **292**; 126857

Wang, Y., J. Luo, Y. Huang, T. Ke, Y. Luo, M. Yang, et al. (2023). Efficient Removal of Phytochrome Using Rice Straw-derived Biochar: Adsorption Performance, Mechanisms, and Practical Applications. *Bioresource Technology*, **376**; 128918

Wijaya, A., P. M. S. B. N. Siregar, A. Priambodo, N. R. Palapa, T. Taher, and A. Lesbani (2021). Innovative Modified of Cu-Al/C (C= Biochar, Graphite) Composites for Removal of Procion Red from Aqueous Solution. *Science and Technology Indonesia*, **6**(4); 228–234

Wu, T., G. Yang, J. Cao, Z. Xu, and X. Jiang (2022). Activation and Adsorption Mechanisms of Methylene Blue Removal by Porous Biochar Adsorbent Derived from Eggshell Membrane. *Chemical Engineering Research and Design*, **188**; 330–341

Zhang, L., Y. Ren, Y. Xue, Z. Cui, Q. Wei, C. Han, and J. He (2020). Preparation of Biochar by Mango Peel and its Adsorption Characteristics of Cd (II) in Solution. *RSC advances*, **10**(59); 35878–35888

Zhang, W., Y. Wang, L. Fan, X. Liu, W. Cao, H. Ai, Z. Wang, X. Liu, and H. Jia (2022). Sorbent Properties of Orange Peel-Based Biochar for Different Pollutants in Water. *Processes*, **10**(5); 856